Advances in Engineering & Scientific Research

Anveshika
Publishing & Informatics

RESEARCH ARTICLE

Frequency Response For Quantum Dot And Well Spin lasers In Dynamical States

Sayedeh Nasrin Hossinimotlagh[1] , Simin Avazzadeh[2]

[1]Department of Physics, Azad Islami University, Shiraz, Iran
[2]Department of Physics, Payame Noor University (PNU) P.O.Box 19395-3697, Tehran, Iran

ABSTRACT

In this paper, we first examine the structure of quantum well and quantum dot lasers. Then, to reduce and eliminate the complexity of the quantum dot laser structure description, we solve the rate equations first in quantum well laser and then in the quantum dot laser for both conventional and spin states. By solving the rate equations, we calculate the dynamic response function of the laser, which can be used to examine the important properties of laser. Finally, according to dynamic response function of quantum well and quantum dot lasers, we examine the bandwidth frequency, peak point frequency and dynamic gain.

KEY WORDS

Quantum ,lasers

HISTORY
Received 18 January 2020
Accepted 13 June 2020
Published 27 June 2020

Volume: 6 Issue: 1

INTRODUCTION

The term spintronic is derivative of resemblance this area to its traditional rival that is, electronic. Two basic properties that are carried by each conduction electron, electrical and magnetic charges that the related are given to quantum spin. In spintronic or electronics based on spin, the quantum modes of the electron spin show their function, that by manipulating this inherent feature, a new generation of electronic devices can be produced. This new technology has important achievements in the department of information and at the same time new research topics in condensed matter physics and materials science[1, 2]. The concept that electric current can be a combination of polarized spin electrons back to 1936, when it was invented by Moot[3]. He found that electric current carriers in a ferromagnetism metal has a pure polarization which is related to conductivity difference of two different spin images and it is known as the two-current model. This model was later expanded by Kampel[4] in 1967 and Ferh and Kampel[5] in 1968. According to Johnson and Silsbee[6] in 1988. Spintronics were built based on the bond between charge and electron spin and the discovery of Giant Magnetic Resistance in 1988 by Fert et al[7]. It was introduced as Spintronic Birth.
The basic studies of spintronics include the research on cases is following:

1. Spin injection: to make a spintronic tool, the first need this is, that system connect that is capable of Production polarized spin electrons current, similar a ferromagnet and a system that is sensitive to electrons spin polarization, created like a non-magnetic material[8].

2. Spin manipulation: this the phrase is of the spin precession movement control, by actions an external electric field that is accompanied with the spin-orbit coupling, spin manipulation involves both population control and spin state control of a set of particles[8].

3. Spin detector: spin detector: a key part of spintronic is that increase the sensitivity of the spin tool to the spin state change[8]. The first attempt to understand spin injection, making an ohmic contact between ferromagnetism and a non-magnetic conductor is problematic due to the different electrical properties of the two materials. In general, the large difference in the density of states at the Fermi level of two materials causes a difference in their conductivity, which is examined in the resistance model equivalent to the connection. The only way to get be useful a spin injection, is to use of a ferromagnetism with 100% polarization, or the resistance of the middle surface must be very large and different for the two spin directions. So that the resistance of the middle surface determines the spin transfer. Eventually, this problem was solved by Firth, Rashba, and Jeffrey, using a selective spin tunnel barrier between ferromagnetic and semiconductor.
The conductivity for up and down spin electrons varies in ferromagnetic materials, therefore, in addition to the electric current in the injection a ferromagnet, a spin current will penetrate into the semiconductor that with itself induces a magnetization during the propagation of the semiconductor spin. One of the important results of spin injection is the accumulation of spin in the connection region. Because in the semiconductor region, the conductivity is the same for the two spin directions, away from the middle surface, inside the non-magnetic region, the current is carried evenly by both spin channels. Because to achieve a steady state, some electrons return during their spin scattering process and enter the opposite spin channel. Note that the only possible interaction for the spin is by a magnetic field that source of can an applied external magnetic field or the produced effective field by the spin-orbit interaction.

Address for correspondence: Sayedeh Nasrin Hossinimotlagh
: Department of Physics, Azad Islami University, Shiraz, Iran

Spin-to-semiconductor electric injection

Another possible spintronic application is the injection of a polarized spin current into a semiconductor system. The polarized spin current, is current which in it a population of a spin specie is more than the other species. Since spin coherence time in semiconductors is much longer than that of spin coherence time in metals, the discussion of spin injection into semiconductors is important. When electrons are injected from a ferromagnetic matter to a nonmagnetic matter, they can keep their spin on a determined distance. The necessary conditions for maintaining this spin polarization are successful spin injections, spin transitions in the semiconductor interior with a multi-micron spin, spin Lifetime greater than 100 ns, and ultimately successful detection. In order to select the suitable material for spin injections, the material should include the polarized spin Carriers Unit Orientation at room temperature. There are many suggestions for electron injectors but the most obvious and definite selection of ferromagnetic materials is due to high temperature Curie, we have chosen their low induction and fast magnetization switching. The induction of a ferromagnetic material is defined as the magnetic field intensity applied to reduce the magnetization of that material to zero, after the sample magnetization has reached saturation. However, there are problems with the use of ferromagnetic materials as spin Injectors to semiconductors. The main problem is the mismatch of conductivity that happens at the interface between ferromagnetic and semiconductor. There are three ways to fix this problem: use of 100% polarized spin material as an injector, use of materials with similar conductivity with semiconductor and use of tunnel barrier[1,2]. First possible solution is the use of semi-metallic ferromagnetism. The idea for semi-metallic ferromagnetic was first proposed by Devere et al. In 1983[9]. Semi-metallic ferromagnetism are materials that have a band gap in a Fermi level for a spin substrate that they make them 100% spin polarized. Although research on semi-metallic ferromagnetism suggests the absence of a system with a spin polarization of 100% at room temperature.

Analytical study of Polarized spin semiconducting lasers

The laser is light amplification by stimulated emission of radiation. The importance of lasers to their widespread use, one of the key characteristics of the laser is the dependence of emitted light to injection. Two polarized and non-polarized spin semiconductor lasers can be separated. Depending on injected the spin carriers are, polarized or unconsolidated. Both lasers have are active region, resonance cavity and carriers injector In polarized spin semiconducting laser, laser operations are directed by charge carriers current in a laser cavity, while the polarization of light emitted by the spins of the carriers is defined. The spin laser heart is a fragment that is called vertical-cavity surface-emitting laser, which is basically a semiconductor laser, the laser beams in the direction z, emitted perpendicular to the sub-layer material on which it grows. Spin electric injections are made using two ferromagnetic connections. Laser resonance cavity consists of two Bragg reflector mirrors parallel to the surface of the sub-layer and laser active region including a well or dot quantum to produce laser light among them. Distributed Bragg Reflector (DBR) mirror consisting of layers with a low and high the refractive coefficient intermittent. Typically, the higher and lower mirrors are p and n types doping materials respectively, which make up a p-n bond. Stimulated emission occurs in the active region the semiconductor Laser of the vertical Cavity Surface Emission.

In the electronically active region in the conduction band, the semiconductor is subjected passage to empty state in the valiancy band that produces photon and leaves the active region. This process of recombination is called electron-hole irradiation. To replenish the electron and hole populations, the charge carriers must be injected into the active region with electrical current. Population inversion is achieved by threshold injecting which the number of electrons in the conduction band is greater than the number of electrons remaining near the top of the valence band. When this happens, the laser cavity losses are defeated and the laser action begins. Threshold current is the current that must be injected to allow laser operations to occur.

If this current is too high, the laser may be impossible for particular applications. The elective rules for optical transitions in quantum well and quantum dot structures depend on participating carriers spin. A spin-up electron of conduction band can only be recombination with a spin-down hole. In this action, a photon is emission with a leftward circular polarization. Conversely, a spin-down electron recombination with a spin-up hole that a photon is emission with a rightward circular polarization. Accordingly, polarized spin semiconductor lasers host two unequal-intensity laser states with left and right circular polarizations. When the semiconductor laser is powered by a polarized spin current, a decrease in threshold current density is observed. Note that if the laser is powered by up-polarized spin current, then the two laser states have equal intensities. It is important to note that electrons spin can be conversion without light emission, and this spin relaxation can limit many of the properties of polarized spin semiconductor laser.

In this paper, we examine the similarities between quantum well (QW) and quantum dot (QD) used as material gain in semiconductor lasers. For active region based on QD, a more complex description is needed. Therefore, mapping between QD and QW lasers has the

ability to easily describe for potential returns. To create such a mapping, our focus is on two conventional lasers (spin un-polarized) and spin-lasers that in it the carriers are spin-polarized. And are injected by circular polarized light or electric injection using magnetic contact. Figure 1 shows a diagram of the conduction band using rate equations for quantum well lasers and quantum dots. In quantum wells, a spinal alignment between injectable carriers leads to the recombination of a number of electron-holes, which causes emitted circular light polarization. S represents the emitted photons with positive and negative helicity, respectively. But the quantum dot laser has several additional processes due to the wetting layer compared to the quantum well laser. The wetting layer (WL) acts as the reservoir of carriers[10-12]. Carriers conquered from WL to QD or, conversely, they can escape from QD to WL.

Bucket model of lasers

One of the most useful comparisons to show the operation of polarized spin semiconductor laser is by the Bucket model, which was previously intended only for unpolarized spin lasers. To describe the Bucket model for polarized spin semiconductor lasers, must first described this model for unpolarized semiconductor lasers. In Figure 2, first showed the bucket model for conventional lasers (spin-unpolarized) and then for polarized spin lasers using rate equations. For conventional lasers, the water level represents the density of the charge carriers, the water faucet represents the carrier injection, the output water represents the emitted light which is the density of the photon, the small leaks on the surface indicate the processes of spontaneous recombination and the large slit on the bucket indicates the lasing threshold (resonance threshold). In low injection (low pumping), the water level is low and some of this water will drip out of the leaks. In this state, there is only insignificant amount of output light. The operation of such laser is like light emissary, spontaneous recombination is a response for light emissary. At high injection (high pumping), the water will reach a large slit and begin to erupt, reaching the lasing threshold (resonance threshold), and Induction recombination dominates the light emission. Excess water will only lead to a small change in water level, but the output will increase rapidly compared to low injection state. At the injection threshold J_T, the spontaneous emission begins and the intensity of the emitted light increases significantly. $J>J_T$ Refers to the inductive recombination leasing performance, which indicates how to work the light emission. The description of section (a) in Figure 2 is similar to Figure 1-a mechanism. In section (b) from Figure 2 illustrates spin laser structural with polarized spin carriers. If you pay attention, the bucket is divided into two halves by the connecting wall. Which indicates the injection of two spin populations, which are filled particularly with hot and cold water, respectively. The openings on connecting wall in Segmentation allow the hot and cold water to mix, the openings on connecting wall in segmentation allow the hot and cold water to mix, which by doing so, it intends to show the spin relaxing that cause mixes the spin-up and spin-down population13. If connecting wall has a small diameter that can be ignorable. The two populations will not be mixed, which corresponds to the time when is unlimited spin relaxation. If the connecting wall is too wide, the immediately unequal populations will be in equilibrium. This leads to carrier polarization of ignorable. With an unequal injection of hot and cold water, the spin injection polarization is defined as follows14: $P_J=((J_+-J_-))/J$ (1)

In it, $J_\pm$ injections are of two spin images that together form the total injection (electric spin injection)$J=J_++J_-$. Δ The difference in levels is cold and hot water (see Figure 2, section b), this leads to three functional region of the carrier and two different leasing thresholds $J_{T1,2}$ 15. Small leaks shows carrier loss through spontaneous recombination, and large slit near the top part indicate the lasing threshold. Total electron density is written as $n=n_++n_-$, total hole density is written as $P=P_++P_-$ and total photon density is written as $S=S^++S^-$.15 In the range of time when spin relaxation is zero, we expect polarized and un-polarized spin semiconductor lasers to behave the same way. Based on the Bucket model, can provide an intuitive understanding of polarized spin semiconductor laser operations. Based on the Bucket model for polarized spin semiconductor lasers, which confirms the existence of two threshold current densities J_{T1} and J_{T2} for carriers with majority and minority spins, for this type of laser, as we said, three functional region are considered. Region I, is region where there is no inductive emission and the laser is off. Region II, is the region where in it carriers have the majority spin lead to lasing (resonance), known as the normalized spin filtering interval. Region III, is the region where carriers both types of spin lead to resonance (lasing).

In low pumping (when both hot and cold water levels are below the large slit), both carriers spin-up and a spin-down are in off region of the light emitting diode (LED), thus, the emitting is insignificant. In higher pumping, the hot water reaches a large slit and erupts as shown in Figure (2, section b). While the amount of cold water that flows out is static and insignificant. This indicates that a region of spin majority is in the leasing state. While the spin minority is still in the LED region, therefore the inductive emission is due to the recombination of the spin majority carriers. By describing section b in Figures 1 and 2, we described the operation of quantum dot lasers with polarized spin carriers as a schematic and a bucket model.

Investigating rate equations in conventional and spin lasers QD and QW:

1. Rate equations in conventional lasers:

In this paper, we first consider rate equations for conventional lasers that used quantum wells as their material gain. Structurally, this laser is similar to Section (a) in Figure 1, also in the previous section structure simulation of this laser with Bucket model was presented (see Figure 2 of Section (a)). Therefore, according to the rate equations, direct relationship between material properties and laser device parameters can be provided. For QW conventional laser, the rate equations are as follows16:

$dn/dt=J-g(n,S)S-R_{sp}$ "(2)"

$ds/dt=\Gamma g(n,S)S+\Gamma\beta R_{sp}-S/\tau_{ph}$ "(3)"

n Demonstrative the carriers density and S is photons density. The optical gain is as follows26:

$g(n,S)=(g0\ (n-n_{tran}))/((1+/S))$ "(4)"

In the paper, g_0 is the gain coefficient reagent17, n_{tran} is the transparency density, and here / is the gain compression factor16. R_{sp} Spontaneous recombination can be dependent on different densities16. Here we focus on the quadratic equations, Bn^2 , which B is temperature dependent constant. Γ Represents the optical confinement factor, β represents the spontaneous emission factor15, 18. τ_{Ph} Indicates the photon lifetime.

According to scrutiny rate equations of (4) and (5) and the optical gain of (6), we find that rate equations are exponentially increased on the variations of t from zero to 50 for n (carrier density), as well as for S (photon density), as shown in Fig. 3, is negligible in relation to t, This means that n is increased more than S versus t.

2. Rate equations in spin lasers:

Now, according to Figures 1 and 2, we describe the rate equations for spin lasers with polarized spin carriers that use quantum dots as material gain. As we have said, since QD spin lasers structure has several processes addition to QW conventional lasers, the rate equations of QD spin laser are more complex than QW conventional laser. The rate equations for QD spin lasers are described as follows21:

$dn_{\pm}/dt=J_{\pm}-g_{\pm}\ n_{\pm}(S^{\pm}\ S)_{\pm}-n_{\pm}+n_{\mp}/(\tau_s^n)-R_{sp}^{\pm}$ "(5)"

$ds^{\pm}/dt=\Gamma g\ (n,S^{\pm})\ S^{\pm}-S^{\pm}/\tau_{ph}-\beta R_{sp\mp}$ "(6)"

In this paper, -/+ subscript (superscript) represent the electron spin (photon helicity). Here, τ_s^n represents the electron spin relaxation time, which for $P_J=0$ in conventional lasers, accordance with spin relaxation $F=(n_{\pm}-n_{\mp})/\tau_S$. Spontaneous recombination rewritten as follows: $R_{sp}^{\pm}=2Bn_{\pm}p_{\pm}$, which $\tau_{sp}\rightarrow 0$ approves hole spin instantaneous relaxation . The hole density is thus eliminated $p_+=p_-=p/2=(n_+ +n_-)/2$, While the results in $R_{sp}^{\pm}=B\ n_{\pm}\ (n_+ +n_-)$ are assumed to charge negative.

In the review of the rate equation for spin lasers according to equation (5) and (6), we find that electrons spin number in positive and negative states increased exponentially, also, Calculation time variations of electrons spin number from electrons helicity number in positive and negative states are higher. Electrons helicity in both states, there is a negligibly increased versus t.

In this section, we compare the rate equations for conventional and spin lasers according to Figures 3,4and Table 1. We find that time variations of electrons spin number (n) in the conventional lasers are higher than spin lasers. But, time variations of electrons helicity (S) in the conventional lasers in relation to spin lasers is decreased by approximately 0.03. The carrier's density in conventional lasers are initially zero and increase with lapse time, and after 25 seconds, the laser emits a constant light. The photons density is such that only increasing it is very small compared to increasing the carriers density. The carrier's density in spin lasers are initially zero and increase with lapse time, and after 5 seconds, the laser emits a constant light. The photons density is such that only increasing it is very small compared to increasing the carriers density similar to conventional lasers.

The net rate of levels occupation probability by electrons and holes in rate equations for QW conventional lasers

Here is we writes briefly time dependence of levels occupying probability by electrons, for QW conventional lasers (according to reference 19, 20):

$(df_w)/dt=I-C+2/K\ E-R_w$ "(7)"

$(df_q)/dt=K/2\ C-E-R_q-G$ "(8)"

$(df_S)/dt=\Gamma_{QD}\ G+\Gamma_{QD}\ \beta R_q-f_S/\tau_{Ph}$ "(9)"

Here, w and q subscripts represent the WL and QD regions (according to Figures 1 and 2), and the S subscript is related to photon (place the laser light is emitted). Here $f_{w,q}$ are indicative the probability of electrons occupying in QD and WL regions, that are written as $f_w=n_w/N_w$ and $f_q=n_q/2N_q$ $0<f_{w,q}<1$. In these, $n_{w,q}$ are indicative the electrons corresponding number, and N_w the states number in WL and N_q are quantum dots number, that each dot has a two fold spin degenerate level. The relationship between the states number in WL and quantum dot number is shown by $K=N_w/N_q$. f_S Is indicative the probability of photon occupation ($f_S=S/2\ N_q$, which S is the number of cavity photons, that doesn't have a high limit. The process of electrons injecting from witting layer region to quantum dot is I=j("1" -f_w), where j is the number of electrons injected into the laser in witting layer state and unit of time. Also, the process of electrons injecting from witting layer region to quantum dot is $C=f_w\ 1-f_q/\tau_c$, and the carrier escape process that is the opposite with capture process, is represented by $E=f_q\ ((1-f_w))/\tau_e$.

In these, τ_c and τ_e are the capture and escape times, respectively.

According to Section B of Figure 2, there are two processes of spontaneous recombination and inductive emission, which show the spontaneous recombination process as $R_\eta=b_\eta f_\eta^2$, and (η=w,q). Thus, the inductive emission process is indicated by $G=g(2 f_q-1) f_S$, where g is not related to gain compression factor and photons occupied, and used in quantum dot lasers. Here the light confinement factor in quantum dot lasers is equal to one (Γ_{QD}=1). In here according to table.2, we reviewed first carrier capture and the escape for QW lasers, then carrier injection and at the end responsible for stimulated emission. We find out that in the states f_w constant and f_q variation between(0-1), carrier escape increase and carrier capture decrease, therefore E and C act on the inverse. Then according to table.2 and Fig.8, we review variation carriers' injection in the states that electrons occupation in the wetting layer f_w constant and j variation. In here we conclude with increase f_w and, carriers' injection J decreases. Next, according to table.2 and Fig.9, we find that responsible for stimulated emission in the state f_q=0, G decreases and f_q=1/2, G is equal to zero, but in the states f_q=1 unlike f_q=0, G increased.

The net rate of levels occupation probability by electrons and holes in rate equations for QW spin lasers

In this part of the paper, the time developments of the occupation probability in rate equations of spin laser are analyzed. Then, by analyzing the difference between the rate equations of spin laser with material gain QW and QD, It is found that the rate equations for quantum dot spin lasers have obvious terms for holes occupation. However, in spin lasers with material gain of quantum well, holes densities can be easily filled or replaced by electron densities. Therefore, for spin lasers with quantum dot material gain, unlike quantum wells, for holes, the spin relaxation time is much faster($\tau_{spw},\tau_{spq}\Delta$ "0). This cause more difficult to analyze spin lasers with quantum dot material gain at steady state, as the holes density associated with rate equations of the quantum dot spin laser does not increase explicitly. Generally the time developments of the levels occupation probability by electrons in rate equations for spin laser, it is as follows:

$$(df_{w\alpha\pm}) dt = I_{\alpha\pm}-C_{\alpha\pm}+2 / \kappa E^{\mp}_{\alpha\pm}-R_{w\pm})f_{wa} \quad "(10)"$$

$$df_{q\mp}/dt=\Delta_{\eta}/2 C_{a\pm}-E_{a\mp}-R_{q\pm}-G_{\pm} f_{qa} \quad "(11)"$$

$$df_S /dt=G_{\pm}+\beta R_{q\pm}-f_S /t_{Ph} \quad "(12)"$$

Here is the subscript a=n,p, which n represents the electrons and p holes, respectively. $I_{a\pm}$=j1-$f_{wa\pm}$))Represents the injection carrier, $C_{a\pm}$ =$f_{wa\pm}$1-$f_{a\pm q}$ /t_c the capture carrier and $E_{a\pm}$=$f_{qa\pm}$1-$f_{wa\pm}$ /t_e in the spin laser. While $j_{a\pm}$=1±P_{ja} j_a represents the number of injected carriers, in which $P_{ja}=j_{a+}-j_{a-}/j_{a+}+j_{a-}$expressive the spin Polarization. The two processes of inductive and spontaneous emission in spin lasers are $G_{\pm}=gf_{qn\pm}+f_{qp\pm}-1)$ $f_{S\pm}$ and $R_{\Delta\pm}=b_\Delta f_{\Delta n\pm} f_{\Delta p\pm}$. In the process of spontaneous emission is Δ=w,q and the spontaneous recombination rate is denoted by b_Δ. In the spontaneous emission, $f_{\Delta a}=f_{\Delta a+}-f_{\Delta a-}$ /$t_{sa\Delta}$ represents the period of the spin relaxation, which $t_{sa\Delta}$ is the spin relaxation time. To calculate and analyze the rate equations in this topic, $t_{Ca}=t_C$، $\tau_{e\alpha}=\tau_e$، $\tau_{sn\eta}=\tau_s$، $\tau_{sp\eta}$= 0 ، β=0 ، J_α=J و $P_{j\alpha}=P_j$are assumed. Occupied electrons are"0"/ $f_{w,q}$)/ 1 , the probability of polarized spin occupancies is shown in three areas: wetting layer $f_{w\alpha\pm}$)=$n_{wa\pm}$/N_{wa}/2, quantum dot $f_{qa\pm}=n_{qa\pm}/N_q$ ،$f_{s\pm}$, and photon production $f_{s\pm}=s_\pm/N_q$.

In this section, we examined the time developments of the occupation probabilities of electrons and holes and photons in the rate equation in both QD and QW lasers for two state conventional (un-polarized) and spin-polarized. In the conventional state according to Figures (5) and (10) and Table.3, we review the time developments of the occupation probabilities electrons in wetting layer (WL) and quantum dot regions, then at end the time developments of the photons production probability. In conventional state, only are electrons and photons occupation probabilities. According to structure of quantum dot lasers, it is expected that the probability of electron occupation in the quantum dot region is higher than the wetting layer region, which according to Figure 10 and study the time developments equations in all three regions, we understand that it is true. Then, the time developments of the occupation probabilities of electrons, holes and photons in the wetting layer and the quantum dots region, according to Figure (10) and Table 3, using the carriers of injection, capture, escape, The excitation and spontaneous emission in the spin state are analyzed and evaluated. Here, we conclude that $f_{\Delta n+}$ the time developments of the occupation probabilities electrons with spin-up in the wetting layer is 0.002 smaller than the spin- down electrons. But 0.002 is larger than the time developments of the occupation probabilities holes with spin-up in the wetting layer. The time developments of the occupation probabilities holes with spin- down in the wetting layer is close to 0.009 from the spin-up state in the holes and near 0.015 from the of occupancy of the electrons in the time developments of the occupation probabilities electrons with up and down spin in wetting layer. Then, we study the time developments of the occupation probabilities electrons and holes with up and down spin at the quantum dot region. Here we find that time developments of the occupation probabilities electrons and holes in the up and down spin increases more than

the time developments of the occupation probabilities electrons and holes in the up and down spin in wetting layer, and it's like conventional lasers close to one. The time developments of the occupation probabilities electrons with up and down spin in wetting layer Both are the same size, and from the time developments of the occupation probabilities, holes with up spin at quantity 0.001 and with down spin is greater quantity 0.002. Finally, with review the time developments of the photons occupation probabilities, we can see which, like conventional lasers, are zero.

DYNAMIC-OPERATION

Since almost many the important and useful properties of lasers are related to their dynamic operation, in this part of the paper, we will examine the dynamic operation mapping in quantum well and quantum dot lasers. The standard method of small signals analysis is used to evaluate the dynamic operation of lasers. According to the harmonic modulation and the standard method of small signals analysis16, the laser frequency response function is as follows, that by the laser frequency response function can be calculated and analyzed of laser dynamic important characteristics16.

$R_{\Delta}=|dS\Delta/dJ\Delta|$ (13)

Here, Δ is modulation frequency, the normalized frequency response function in quantum well lasers according to Equation 13 and small signals analysis is as follows:

$|R(\Delta)/R(0)\ QW=\Delta_R^2/\Delta_R^2-\Delta^2+\Delta^2\Delta^{2\ 1/2}$ (14)

This response function is useful in quantum well lasers in expressing damping coefficient. Which $\Delta\approx 2Bn_T + K_{\omega R}^2/2p^2$ represents the damping coefficient21, 22, factor K is an important parameter to express the characteristics of the laser because it determines the operation limit at high speed of lasers that is how it is written $K\approx 4\pi^2 + (_{Ph}\tau/g_0)$. And ω_R is the relaxation oscillation frequency that is how it is written $\omega_R^2(g_0 s_0)/[\tau_{ph}(1+\varepsilon s_0)]$.

In the square of the frequency response function of QW laser, the laser bandwidth is reduced by 3db, where of the laser bandwidth frequency with w is shown. In the event that when the damping is weak $\omega_R \gg \gamma$, the bandwidth frequency of quantum well lasers Dependent and related to relaxation oscillation frequency and peak point frequency . The peak point frequency show with $\omega_{peak}^2 = \omega_R^2 - \gamma^2/2$. In general , in these equations it is assumed that $\varepsilon \ll g_0/(2Bn_T)$ .The bandwidth frequency is as follows32 , 32 :

$\omega_{3dB}^2 = \omega_{Peak}^2 + (\omega_{Peak}^4 + \omega_R^4)^{1/2}$ (15)

The maximum bandwidth frequency is obtained by explaining the monotone reduction of the frequency response function for relaxation frequency square $\omega_R^2=\omega^2/2$. Now the frequency response function for quantum dot lasers is written according to the quantum well response function and the assumption $\omega r \ll 1/(_c\tau)$ that $\tau_c \approx (\tau_c)/1-f_{q0}$ is the capture time of effective factor:

$|R(\omega)/R(0)|_{QD} \approx 1+\omega^2 \tau_C'^{2\ -1/2} / |R(\omega)/R(0)|_{QW}$ (16)

Here, for dynamic operation mapping, first we explanation the normalized frequency response function in quantum well lasers. Which is shown in Figure 11. In Fig. 11, we have investigated different states of the normalized frequency response function in QW lasers when ω is constant, that the response function at the frequency zero does not respond properly, but shows its peak position at the remaining frequencies (See Figure 11). Then, we examine the peak point frequency and the bandwidth frequency, which consider both in the two modes: 1) the fixed damping factor 2) the constant relaxation oscillation frequency. In the case of constant damping factor γ, the peak position frequency and bandwidth frequency both increase. The peak position frequency with relaxation oscillation frequency increases exponentially downward, increasing (See Figure 12). But, the bandwidth frequency with relaxation oscillation frequency increases exponentially upward increases (See Figure 13). Then, in the state that is constant relaxation oscillation frequency, peak position frequency and bandwidth frequency are both exponentially downtrend, The peak position frequency according to Fig. 12, with increasing damping factor in different states of the constant relaxation oscillation frequency each graph, reaches a fixed point on the damping curve (see Fig.12). But, bandwidth frequency with increasing damping factor in different states relaxation oscillation frequency each graph, in the end reaches a fixed downtrend (see Fig. 13). According to Fig. 14, increases the damping factor in the different constant frequencies by the normalized frequency response function exponentially increases, but in the state that ω=20, such as the yellow graph of the Fig.14 within a certain range of the axis, has An uptrend and then In the following this uptrend is less, So that almost graphing becomes monotonic, with increasing frequencies, for example ω=40 ,60, As green and red graphs of the fig.14, we have an increase in the beginning, but in the middle of this figures, we encounter decreasing and increasing oscillation, and at the end ω=80 ,100, like blue and brown graphs of the fig.14, Overall, we see an uptrend. But in the state that consider the constant damping factor, in all states, by increasing relaxation oscillation frequency of the normalized frequency response function in quantum dot lasers exponentially decreases.

The bandwidth frequency of quantum dot lasers compared to quantum wells is as follows:

$(1+\omega_{3dB}^{2}\tau_C'^{2})[(\omega_r^{2}-\omega_{3dB}^{2})+\omega_{3dB}^{2}\gamma_{QD}^{2}]=2\omega_r'^{4}$

When capture time is short enough $\tau_c \rightarrow 0$, the dynamic response of quantum dot laser reaches its maximum23 , 24 . As mentioned earlier , recover the dynamics of quantum dot lasers is done by quantum well rate equations . Now , considering the dynamic response function , we calculate and examine the dynamic gain :

$\Delta_d \approx g_0 (\sqrt{2}/(\omega_{3dB}^{max})-\tau_{Ph})$

Where the subscript d refers to the dynamical response. The dynamic gain after carrier capture τ_c=2Ps, it shows Less than 3% error.

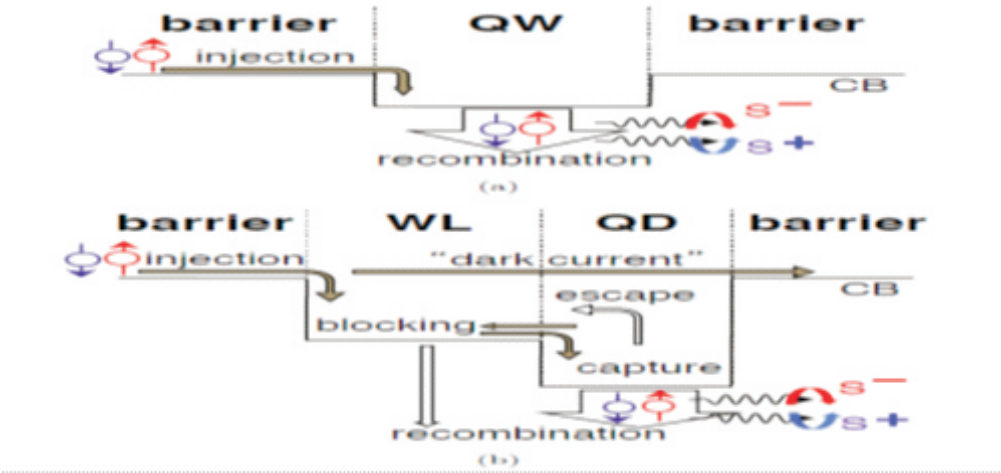

Figure : 1 Conduction band diagram in semiconductor lasers. (a) Quantum well (QW) laser. (b) Quantum dot (QD) laser.

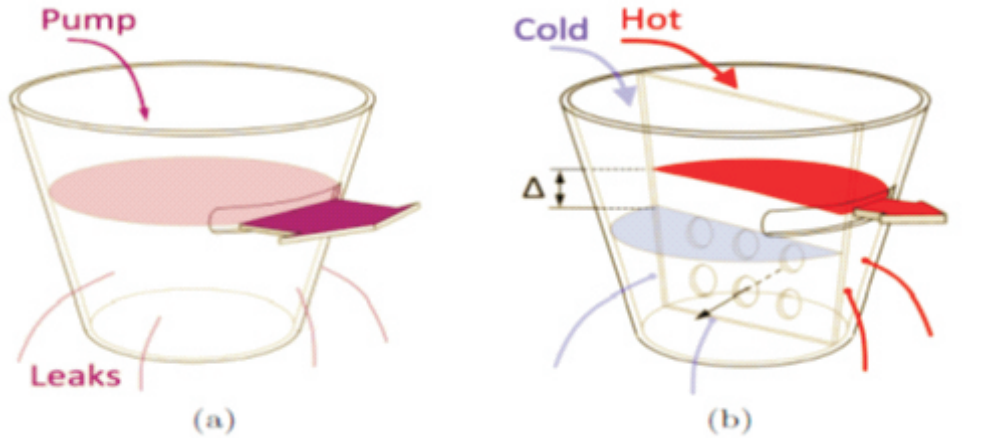

Figure :2 Bucket model of lasers. a) Bucket model simulation for conventional lasers. b) Bucket model simulation for spin lasers

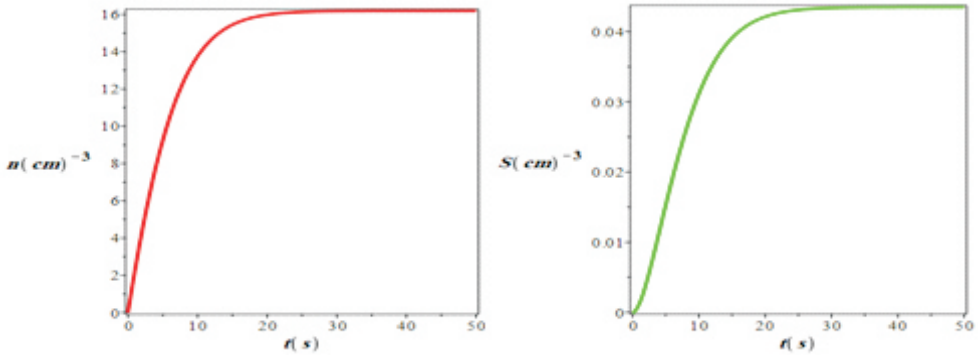

Figure : 3 Calculation time variations of rate equations for carrier and photon density, n and S in conventional lasers.

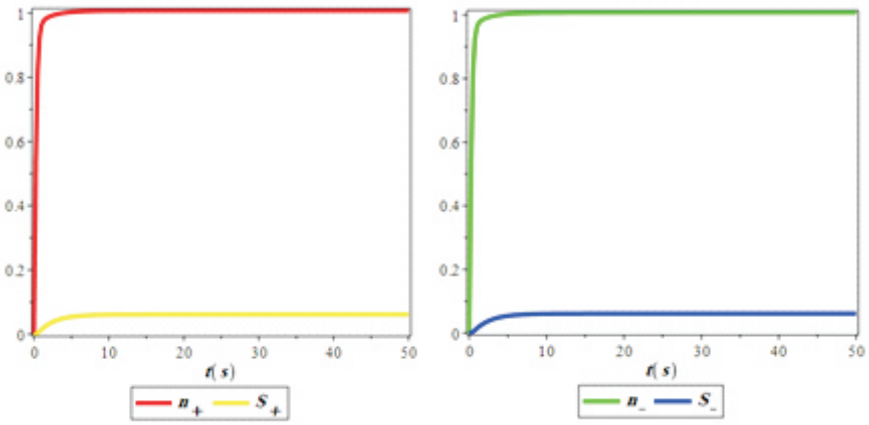

Figure : 4 Calculation time variations of rate equations for carrier and photon density, n and S in spin lasers.

Table :1 Investigation numerical values of time variations of Rate equation for convention and spin lasers.

t	0	10	20	30	40	50
n	0	13.761	15.981	16.176	16.190	**16.191**
n_+	0	1.007	1.007	1.007	1.007	**1.007**
n_-	0	1.007	1.007	1.007	1.007	**1.007**
S	0	0.031	0.042	0.043	0.043	**0.043**
S_+	0	0.060	0.061	0.061	0.061	**0.061**
S_-	0	0.060	0.061	0.061	0.061	**0.061**

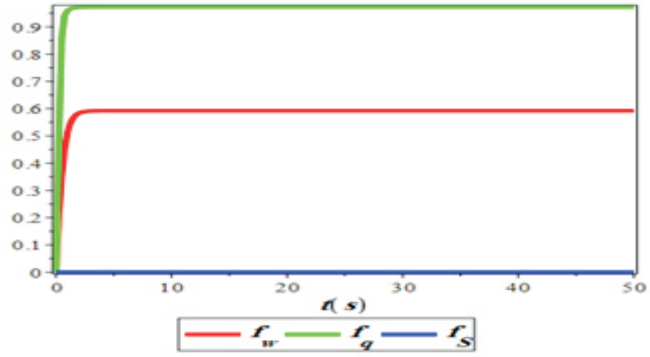

Figure : 5 Calculation time variations of rate equations for carrier and photon density, n and S in spin lasers.

Table :2 Investigation numerical values of injection, capture, escape, and the stimulated emission carriers.

f_q	f_w	C	E	J	f_w	I	f_s	f_q	G
0	0	0	0	0	0	0	0	0	0
$\frac{1}{2}$		0	$\frac{1}{2}$	1		1	$\frac{1}{2}$		−0.008
1		0	1	2		2	1		−0.0016
0	$\frac{1}{2}$	0.25	0	0	$\frac{1}{2}$	0	0	$\frac{1}{2}$	0
$\frac{1}{2}$		0.12	$\frac{1}{4}$	1		$\frac{1}{2}$	$\frac{1}{2}$		0
1		0	$\frac{1}{2}$	2		1	1		0
0	1	0. 5	0	0	1	0	0	1	0
$\frac{1}{2}$		0.25	0	1		0	$\frac{1}{2}$		0.008
1		0	0	2		0	1		0.0016

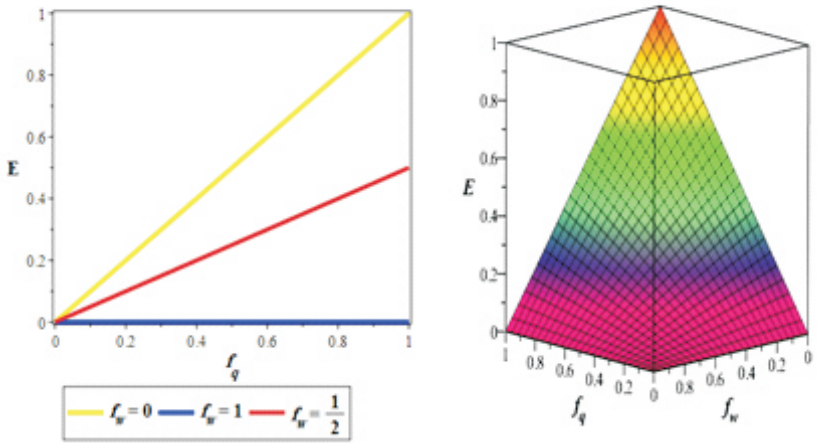

Figure :6 Variation carriers escape versus electron occupation in the wetting layer (WL) and quantum dot regions (QD).

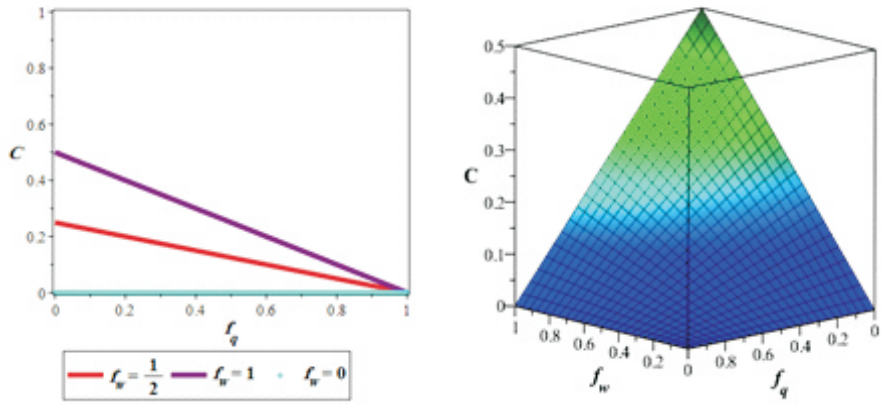

Figure : 7 Variation carriers captuer versus electron occupation in the wetting layer (WL) and quantum dot regions (QD).

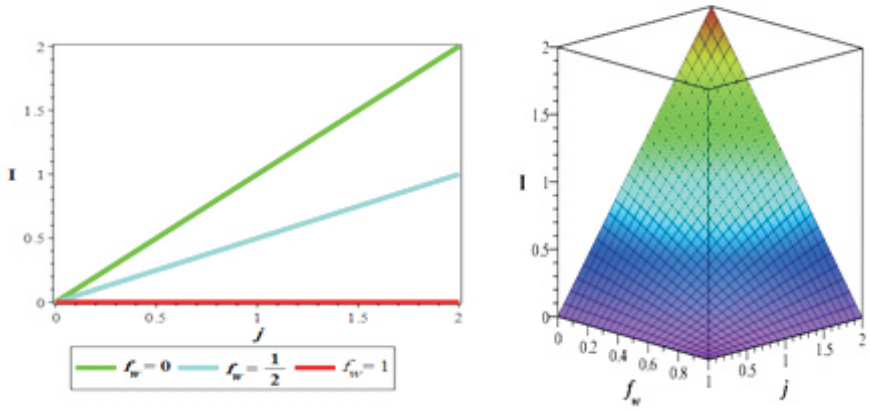

Figure : 8 Variation carriers injection versus electron occupation in the wetting layer (WL) and number of carriers (electrons) injected into the laser per WL state and unit time (j).

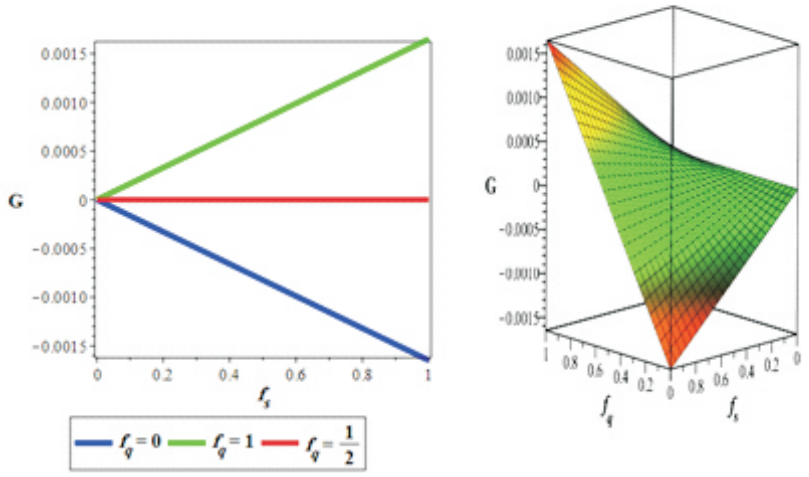

Figure : 9 Variation responsible for stimulated emission versus electron occupation in the quantum dot regions (QD) and photon occupancy.

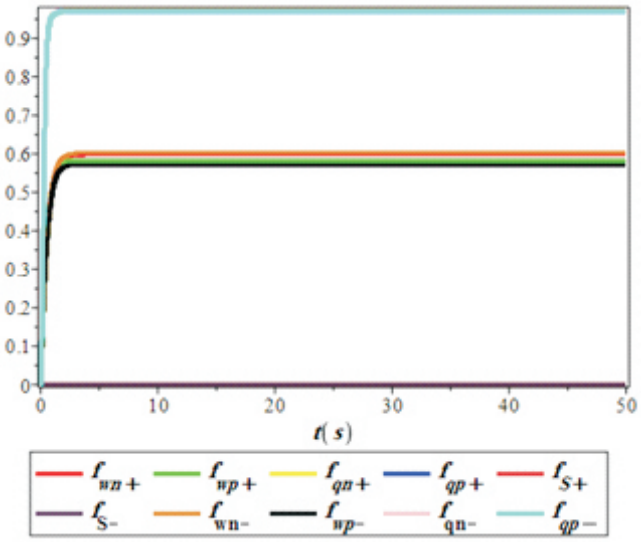

Figure : 10 The time developments of the occupation probability in rate equations of spin laser .

Table :3 Investigation numerical values of the temporal evolution of the occupation probabilities in the RE model for conventional and spin lasers.

t	0	10	20	30	40	50
f_{ω}	0	0.591	0.591	0.591	0.591	0.591
$f_{\omega n+}$	0	0.593	0.593	0.593	0.593	0.593
$f_{\omega n-}$	0	0.595	0.595	0.595	0.595	0.595
$f_{\omega p+}$	0	0.591	0.591	0.591	0.591	0.591
$f_{\omega p-}$	0	0.580	0.580	0.580	0.580	0.580
f_{q}	0	0.972	0.972	0.972	0.972	0.972
f_{qn+}	0	0.973	0.973	0.973	0.973	0.973
f_{qn-}	0	0.973	0.973	0.973	0.973	0.973
f_{qp+}	0	0.972	0.972	0.972	0.972	0.972
f_{qp-}	0	0.971	0.971	0.971	0.971	0.971
f_{s}	0	0	0	0	0	0
f_{s+}	0	0	0	0	0	0
f_{s-}	0	0	0	0	0	0

Table : 4 The QD laser parameters are t_{Ph}=2ps, b_q t_{Ph}=0.01, , b_w t_{Ph}=2.33, gt_{Ph}=2, Δ=100 and t_e=1 ns (Ref.13, 19).

Q W parameters	$\tau_c = 0$	$\tau_c = 2ps$	U nit
ϵ_s	0	1.62×10^{-14}	cm^3
ϵ_d(Ref.50)	0	6.39×10^{-15}	cm^3
g_0	1.90×10^{-3}	1.65×10^{-3}	$cm^3 S^{-1}$
n_{tran}	3.50×10^{16}	3.58×10^{16}	cm^3
B	143×10^{-7}	1.28×10^{-7}	$cm^3 S^{-1}$
τ_{Ph}	2		
Γ	0.03		

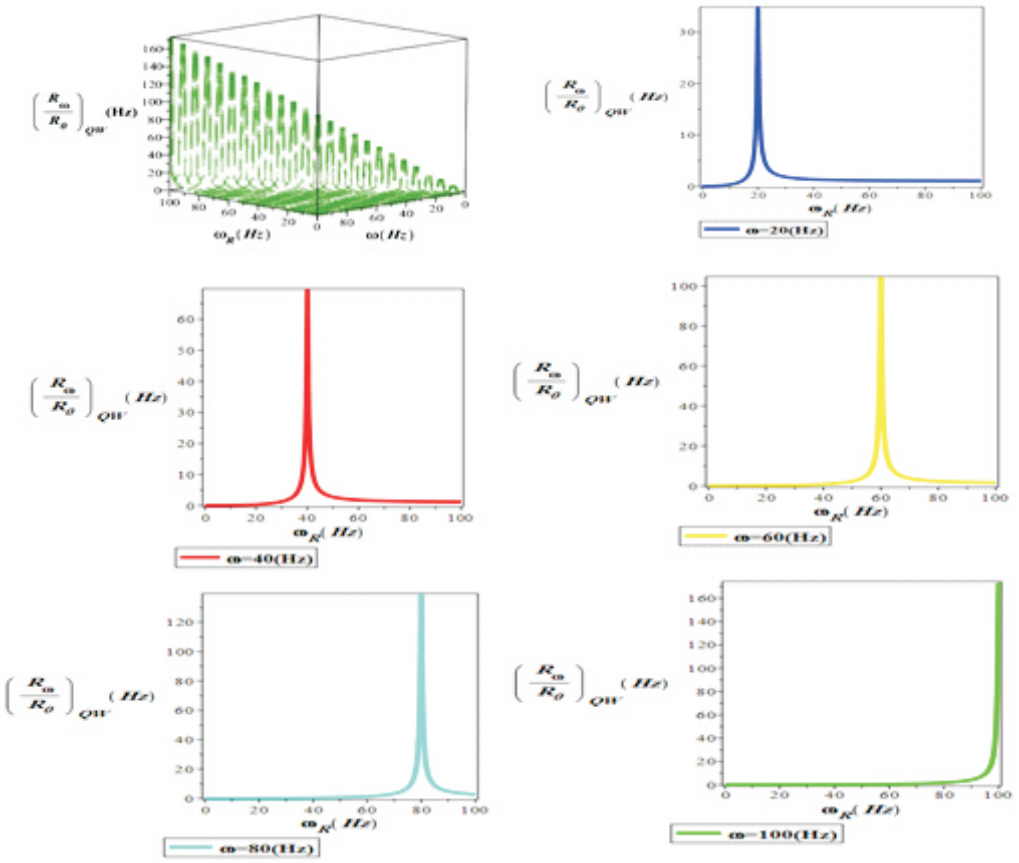

Figure :11 Variation normalized frequency response function in the wetting layer versus frequency and relaxation oscillation frequency.

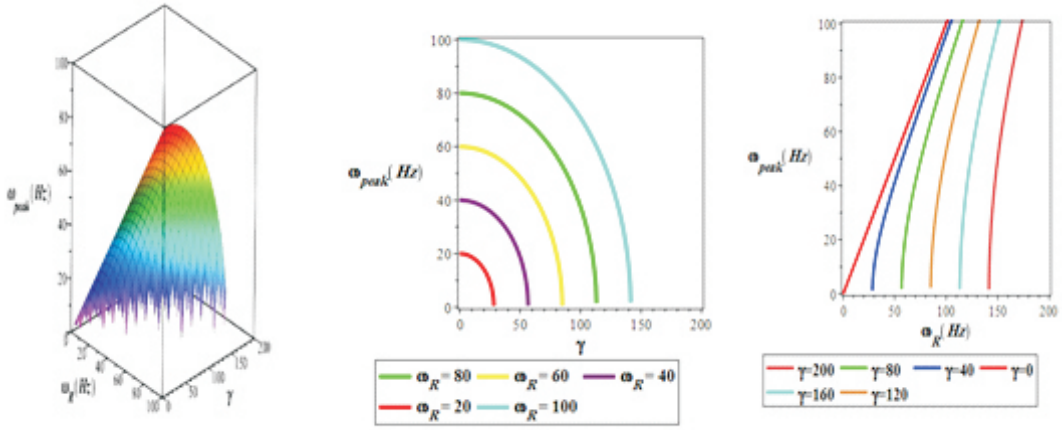

Figure : 12 Variation peak position frequency versus relaxation oscillation frequency and damping factor.

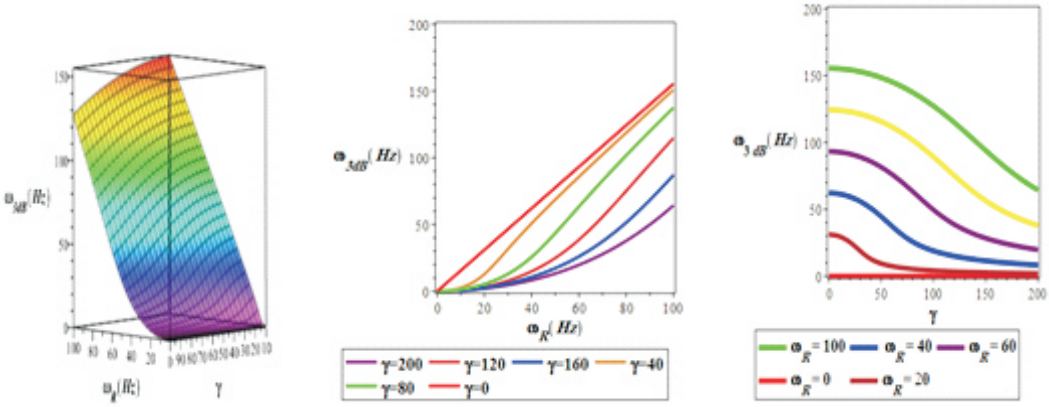

Figure : 13 Variation bandwidth frequency versus relaxation oscillation frequency and damping factor.

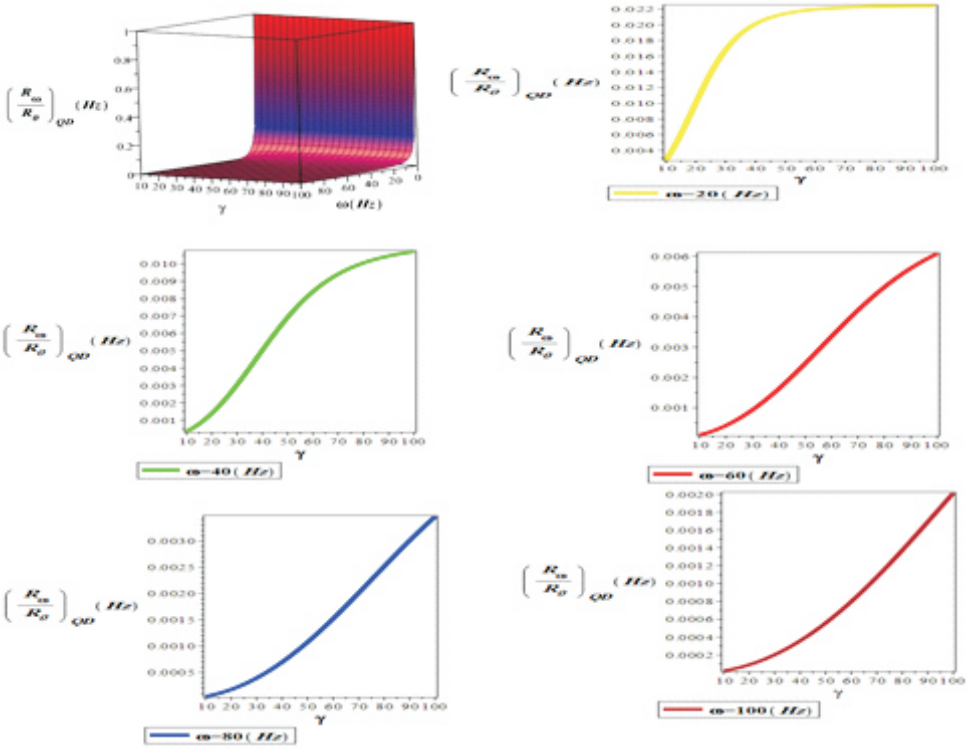

Figure : 14 Variation frequency response function the QD laser versus frequency and relaxation oscillation frequency.

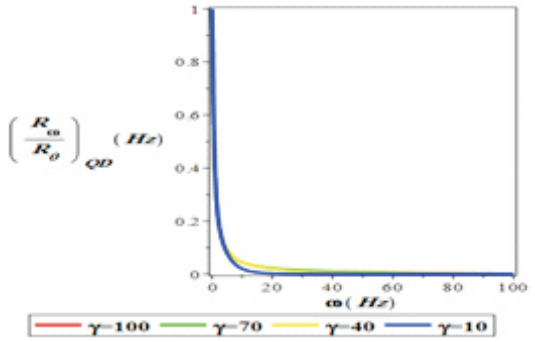

Figure : 15 Variation frequency response function the QD laser versus frequency and damping factor.

Table :5 Calculates numerical values the normal frequency response function in QW laser.

ω_R	ω	$\left\|\frac{R(\omega)}{R(0)}\right\|_{QW}$
0	20	0
20		34
40		1.30
100		1.04
0	40	0
40		68
60		1.78
100		1.19
0	60	0
60		103
80		2.22
100		1.56
0	80	0
80		138
100		2.77
0	100	0
100		173

Table : 6 Calculates numerical values the normal frequency response function in QD laser.

ω / γ	2 0	40	60	80	100
10	0.002	3.5×10^{-4}	1.04×10^{-4}	4.30×10^{-5}	2.24×10^{-5}
40	0.019	0.005	0.0016	7×10^{-4}	3.6×10^{-5}
70	0.022	0.009	0.004	0.002	0.0010
100	0.022	0.010	0.006	0.003	0.002

Table : 7 Calculates numerical values the normal frequency response function in QD laser.

ω \ γ	10	40	80	100
20	0.002	0.019	0.022	0.022
40	3.5×10^{-4}	0.005	0.009	0.010
60	1.04×10^{-4}	0.0016	0.004	0.006
80	4.30×10^{-5}	7×10^{-4}	0.002	0.003
100	2.24×10^{-5}	3.6×10^{-5}	0.0010	0.002

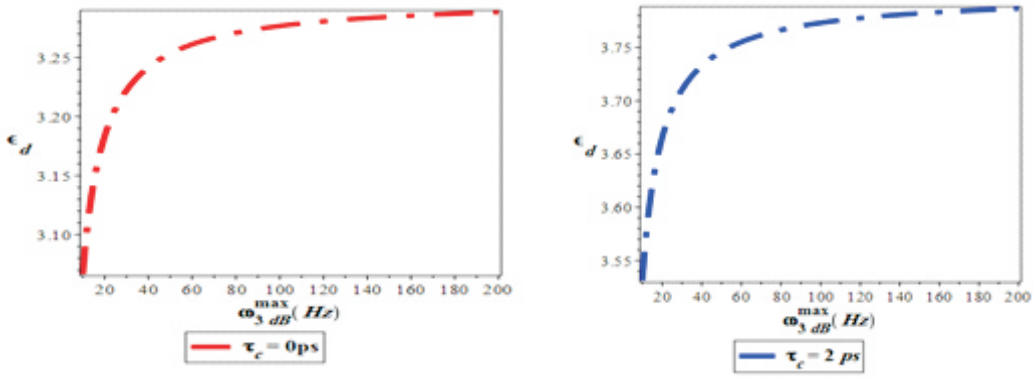

Figure : 15 Reviwe Variation dynamical gain versus maximum bandwidth frequency in the τ_c=0 and 2.

Table : 8 Calculates numerical values the dynamical gain calculations in the capture time.

ω_{3dB}^{max} \ ϵ_d	$\tau_c = 0$	$\tau_c = 2$
10	3.53	3.06
50	3.74	3.25
100	3.77	3.27
150	3.78	3.28
200	3.78	3.28

CONCLUSIONS

In this paper, the QD and QW lasers rate equations from conventional lasers to spin lasers were published, and according to rate equations, we investigated dynamic-operation for both QD and QD lasers, which, according to method standard of small-signal analysis, here we get the system response function for both lasers. As a result, we find that the damping factor on the response function is more effective than frequency. In this paper, we reduce the complexity of quantum dot laser structure to some extent based on the analysis of rate equations in both normal and spin modes.Finally, we obtain dynamic gain at t_c=0,2. Dynamic gain gives a less than 3% error witht_c=2ps, and we compared with the laboratory state, which dynamic gain gives a less than 3% error with t_c=2ps.25

REFRENCES

[1]. Spintronic devices, Alessandro Chiolerio , PhD Thesis, (2009)

[2]. Development of organic-based thin film magnets for spintronics ,Elin Carlegrim,Linkoping Studies in Science and Technology, Dissertation No. 1317(2010).

[3]. 3.RD Moot, R Conover - The Planners' Journal, 1936 - Taylor & Francis.

[4]. I.A. Campbell, A. Fert, R Pomeroy - Philosophical Magazine, 1967 - Taylor & Francis.

[5]. Fert, I.A. Campbell - Physical Review Letters, 21,1190 – Published14 October 1968 – APS.

[6]. Middle Triassic Scleractinia from the Cracow-Silesia region, Poland. Acta Palaeont. Polonica, 33, 2, 91-121, 1988.

[7]. Kazarinov, R.F; Suris, R.A. (April 1971). "Possibility of amplification of electromagnetic waves in a semiconductor with a superlattice". Fizika i Tekhnika Poluprovodnikov 5 (4): 797–800.

[8]. Quantum theory of spintronics in magnetic nanostructures, J. Mathon, A.Umerski ,Handbook of Theoretical and Computational Nanotechnology, Volume 1, Pages(1-70),(2005).

[9]. DeVere, Stephen P.; Scott, Clifford D.; Shulby, William L. 1983, Vol. 10 Issue 1, p185-190. 6p. 8 Charts.

[10]. J. Huang and L. W. Casperson, Opt. Quant. Electron. 25, 369 (1993).

[11]. Zuti´c, J. Fabian, and S. C. Erwin, Phys. Rev. Lett. 97, 026602 (2006).

[12]. S. F. Yu, Analysis and Design of Vertical Cavity Surface Emitting Lasers (Wiley, New York, 2003).

[13]. R. Al-Seyab, D. Alexandropoulos, I. D. Henning, and M. H. Adams, IEEE Photonics J. 3, 799 (2011).

[14]. Y. B. Ezra, B. I. Lembrikov and M. Hardim, IEEE J. Quantum Electron. 45, 34 (2009).

[15].Vurgaftman, M. Holub, B. T. Jonker, and J. R. Mayer, Appl. Phys. Lett. 93, 031102 (2008).

[16].A. Sellers, H. Liu, K. Groom, D. Childs, D. Robbins, T. Badcock, M. Hopkinson, D. Mowbray, and M. Skolnick, Electron. Lett. 40, 1412 (2004).

[17]. Zuti´c, J. Fabian, and S. Das Sarma, Phys. Rev. B 64, 121201® (2001).

[18]. M. Oestreich, J. Rudolph, R. Winkler, and D. H¨agele, Superlattices Microstruct. 37, 306 (2005).

[19]. J. Lee, W. Falls, R. Oszwa ldowski, and I. ˇZuti´c, Spin modulation in lasers, Appl. Phys. Lett. 97, 041116 (2010).

[20]. D. Basu, D. Saha, C. C. Wu, M. Holub, Z. Mi and P.Bhattacharya, Appl. Phys. Lett. 92, 091119 (2008).

[21]. S. Hallstein, J. D. Berger, M. Hilpert, H. C. Schneider, W. W. R¨uhle, F. Jahnke, S. W. Koch, H. M. Gibbs, G. Khitrova, M. Oestreich, Phys. Rev. B 56, R7076 (1997).

[22]. H. Soldat, M. Li, N. C. Gerhardt, M. R. Hofmann, A. Ludwig, A. Ebbing, D. Reuter, A. D.Wieck, F. Stromberg, W. Keune, and H. Wende, Appl. Phys. Lett. 99, 051102 (2011).

[23].E. D. Fraser, S. Hegde, L. Schweidenback, A. H. Russ, A. Petrou, H. Luo, and G. Kioseoglou, Appl. Phys. Lett. 97, 041103 (2010).

[24]. R. Oszwa ldowski, C. Gothgen, and I. ˇZuti´c, Phys. Rev. B 82, 085316 (2010).

[25]. S. A. Crooker, E. S. Garlid, A. N. Chantis, D. L. Smith, K. S. M. Redd, Q. O. Hu, T. Kondo, and C. J. Palmstrom, and P. A. Crowell, Phys. Rev. B 80, 041305 ® (2009).